High-precision charm-quark mass and QCD coupling from current-current correlators in lattice and continuum QCD

I. Allison,[1] E. Dalgic,[2] C. T. H. Davies,[3] E. Follana,[4] R. R. Horgan,[5] K. Hornbostel,[6] G. P. Lepage,[7,*] C. McNeile,[3] J. Shigemitsu,[4] H. Trottier,[2] R. M. Woloshyn,[1] K. G. Chetyrkin,[8] J. H. Kühn,[8] M. Steinhauser,[8] and C. Sturm[9]

(HPQCD Collaboration)

[1]*TRIUMF, 4004 Wesbrook Mall, Vancouver, BC, V6T 2A3, Canada*
[2]*Physics Department, Simon Fraser University, Vancouver, British Columbia, Canada*
[3]*Department of Physics and Astronomy, University of Glasgow, Glasgow G12 8QQ, UK*
[4]*Physics Department, The Ohio State University, Columbus, Ohio 43210, USA*
[5]*Department of Applied Mathematics and Theoretical Physics, Cambridge University, Wilberforce Road, Cambridge CB3 0WA, UK*
[6]*Southern Methodist University, Dallas, Texas 75275, USA*
[7]*Laboratory for Elementary-Particle Physics, Cornell University, Ithaca, New York 14853, USA*
[8]*Institut für Theoretische Teilchenphysik, Universität Karlsruhe, D-76128 Karlsruhe, Germany*
[9]*Physics Department, Brookhaven National Laboratory, Upton, New York 11973, USA*

(Received 19 May 2008; revised manuscript received 8 August 2008; published 29 September 2008)

We use lattice QCD simulations, with MILC gluon configurations and HISQ c-quark propagators, to make very precise determinations of moments of charm-quark pseudoscalar, vector and axial-vector correlators. These moments are combined with new four-loop results from continuum perturbation theory to obtain several new determinations of the $\overline{\mathrm{MS}}$ mass of the charm quark and of the $\overline{\mathrm{MS}}$ coupling. We find $m_c(3\ \mathrm{GeV}) = 0.986(10)\ \mathrm{GeV}$, or, equivalently, $m_c(m_c) = 1.268(9)\ \mathrm{GeV}$, both for $n_f = 4$ flavors; and $\alpha_{\overline{\mathrm{MS}}}(3\ \mathrm{GeV}, n_f = 4) = 0.251(6)$, or, equivalently, $\alpha_{\overline{\mathrm{MS}}}(M_Z, n_f = 5) = 0.1174(12)$. The new mass agrees well with results from continuum analyses of the vector correlator using experimental data for e^+e^- annihilation (instead of using lattice QCD simulations). These lattice and continuum results are the most accurate determinations to date of this mass. Ours is also one of the most accurate determinations of the QCD coupling by any method.

DOI: 10.1103/PhysRevD.78.054513 PACS numbers: 11.15.Ha, 12.38.Aw, 12.38.Gc

I. INTRODUCTION

Precise values for the QCD coupling $\alpha_{\overline{\mathrm{MS}}}$ and the charm-quark's mass m_c are important for high-precision tests of the standard model. Some of the most accurate mass determinations currently come from zero-momentum moments of current-current correlators built from the c quark's electromagnetic current (see, for example, [1,2]). Low moments are perturbative and have long been known through three-loop order [3–5]. New techniques have recently extended these results to much higher moments [6,7] and, in some cases, to four-loop order [8–10]. These moments can be estimated nonperturbatively, using dispersion relations, from experimental data for the electron-positron annihilation cross section, $\sigma(e^+e^- \to \gamma^* \to X)$. The c quark's mass is extracted by comparing the perturbative and experimental determinations.

In this paper we show how to compute such moments directly using accurately tuned, highly realistic numerical simulations of QCD in the lattice approximation [11]. As we will show, the correlator moments obtained nonperturbatively from such simulations can be used in place of data from e^+e^- annihilation to obtain new, percent-accurate determinations of the c quark's mass. With lattice QCD, it is also possible to replace the electromagnetic current in the correlator by the pseudoscalar operator $m_c\bar{\psi}_c\gamma_5\psi_c$, thereby providing a completely new set of mass determinations and an important cross-check on the entire methodology.

In fact the pseudoscalar correlators are particularly easy to simulate, and there are no renormalization factors required since the corresponding axial-vector current is partially conserved in our lattice formalism. Consequently these correlators give our most accurate masses. They also give very accurate values for the QCD coupling, when combined with our new four-loop results from perturbation theory.

In Sec. II we describe how to compute pseudoscalar correlators and their moments using lattice QCD. We discuss techniques for reducing lattice artifacts in Sec. III, and present new determinations of the c-quark mass and QCD coupling from our lattice "data" in Sec. IV. In Sec. V we extend our analysis to include vector and axial-vector correlators. We summarize our main results in Sec. VI.

*g.p.lepage@cornell.edu

 © 2008 The American Physical Society

In the Appendix we review the continuum perturbation theory needed for this analysis, including new four-loop results for the pseudoscalar and vector cases.

II. LATTICE QCD AND PSEUDOSCALAR CORRELATORS

Few-percent accurate QCD simulations have only become possible in the last few years (see, for example, [12,13]), and accurate simulations of relativistic c quarks only in the past year—with the new highly improved staggered quark (HISQ) discretization of the quark action [14,15] that we use here. A lattice QCD simulation proceeds in two steps. First the QCD parameters—the bare coupling constant and bare quark masses in the Lagrangian—must be tuned. Then the tuned simulation is used to compute vacuum matrix elements of various quantum operators from which physics is extracted. An obvious approach to the tuning is to choose a lattice spacing a, and then tune each of the QCD parameters so that the simulation reproduces the experimental value for a corresponding physical quantity that is well measured. It is more efficient, however, to first choose a value for the bare coupling and then adjust the lattice spacing and bare masses to give physical results.

In the simulations used here, we set the lattice spacing to reproduce the correct $\Upsilon' - \Upsilon$ meson mass difference in the simulations [16], while we tune the u/d, s, c,and b masses to give correct values for m_π^2, $2m_K^2 - m_\pi^2$, m_{η_c}, and m_Υ, respectively. (For efficiency we set $m_u = m_d$; this leads to negligible errors in the analysis presented here.) The important parameters for the particular simulations used in this paper are listed in Table I; further details can be found in [12,15]. Once these parameters are set, there are no further physics parameters, and the simulation will accurately reproduce QCD physics for momenta much smaller than the ultraviolet (UV) cutoff ($\Lambda \sim \pi/a$).

We have tested these simulations extensively (see, for example, [12–16]) and, in particular, we have done very precise tests for the charm-quark physics most relevant to this work. These demonstrate, for example, that our simulations reproduce the low-lying spectrum, including spin structure, of both charmonium and heavy-light mesons (D and D_s) to within our simulation uncertainties (a few percent or less) [14,15].

Given a tuned simulation, it is straightforward to calculate correlators of the sort used to determine m_c. The simplest of these is for the c quark's pseudoscalar density, $j_5 \equiv \bar{\psi}_c \gamma_5 \psi_c$:

$$G(t) \equiv a^6 \sum_{\mathbf{x}} (am_{0c})^2 \langle 0 | j_5(\mathbf{x}, t) j_5(0,0) | 0 \rangle \qquad (1)$$

where m_{0c} is the c quark's bare mass (in the lattice Lagrangian). Here time t is Euclidean, and the sum over spatial position $\mathbf{x}$ sets the total three momentum to zero. Note that $G(t) = G(T - t) = G(T + t)$ where T is the temporal length of the lattice.

We include two factors of am_{0c} in the definition of $G(t)$ so that $G(t)$ becomes independent of the UV cutoff as $a \to 0$ [18]. Consequently the lattice and continuum $G(t)$'s become equal in this limit. Moments G_n are trivially computed:

$$G_n \equiv \sum_t (t/a)^n G(t), \qquad (2)$$

where, on our periodic lattice [19],

$$t/a \in \{0, 1, 2 \ldots T/2a - 1, 0, -T/2a + 1 \ldots -2, -1\}. \qquad (3)$$

The cutoff independence of $G(t)$ implies that

$$G_n = \frac{g_n(\alpha_{\overline{\rm MS}}(\mu), \mu/m_c)}{(am_c(\mu))^{n-4}} + \mathcal{O}((am_c)^m) \qquad (4)$$

for $n \geq 4$, where $m_c(\mu)$ is the $\overline{\rm MS}$ mass at scale μ and g_n is dimensionless. The c mass can be determined from moments with $n \geq 6$ given G_n from lattice simulations and g_n from perturbation theory (see the Appendix), while the QCD coupling can be determined from the dimensionless moment G_4. This assumes that perturbation theory is applicable, which should be the case for small enough n.

Note that here and elsewhere in this paper we omit annihilation contributions from $c\bar{c} \to$ gluons $\to c\bar{c}$. This is allowed provided we omit the same contributions from perturbation theory. Annihilation contributions to the nonperturbative part of our analysis would be negligible (for example, they shift the η_c mass by approximately 2.4 MeV, which is less than 0.1% [14,20]).

TABLE I. Parameters for the QCD simulations used in this paper. The inverse lattice spacing a^{-1} is in units of $r_1 = 0.321(5)$ fm [16], defined in terms of the static-quark potential [17]. L and T are the spatial and temporal size of the lattices used for each set of gluon configurations. The configurations used here were generated by the MILC collaboration [17] with u, d, and s sea quarks. The u and d masses are set equal to $m_{u/d}$. The sea-quark masses are given in the standard MILC notation which includes a factor of the (plaquette) tadpole factor u_0.

Set	r_1/a	$au_0m_{0u/d}$	au_0m_{0s}	am_{0c}	u_0	L/a	T/a
1	2.133(14)	0.0097	0.048	0.850	0.860	16	48
2	2.129(12)	0.0194	0.048	0.850	0.861	16	48
3	2.632(13)	0.0050	0.050	0.650	0.868	24	64
4	2.610(12)	0.0100	0.050	0.660	0.868	20	64
5	2.650(8)	0.0200	0.050	0.648	0.869	20	64
6	3.684(12)	0.0062	0.031	0.430	0.878	28	96
7	3.711(13)	0.0124	0.031	0.427	0.879	28	96
8	5.277(16)	0.0036	0.018	0.280	0.888	48	144

III. QCD SIMULATIONS

A. Reduced moments

The biggest challenge when using lattice QCD to produce c-quark correlator moments is controlling: (1) $\mathcal{O}((am_c)^n)$ errors caused by the lattice approximation; and (2) tuning errors in the QCD parameters, and especially in the lattice spacing and the c-quark's bare mass. We reduce each of these sources of error by making two modifications to the moments.

First we replace G_n by

$$\frac{G_n}{G_n^{(0)}} = \frac{g_n}{g_n^{(0)}}\left(\frac{m^{(0)}_{\mathrm{pole},c}}{m_c(\mu)}\right)^{n-4} + \mathcal{O}((am_c)^m\alpha_s) \tag{5}$$

where $G_n^{(0)}$ is the nth moment of the correlator to lowest order in lattice QCD perturbation theory [21], $g_n^{(0)}$ is the lowest-order part of g_n in continuum perturbation theory, and exponent $m = 2, 4\ldots$. The lowest-order on shell or "pole" mass of the c-quark sets the mass scale in the lowest-order lattice moments

$$G_n^{(0)} = \frac{g_n^{(0)}}{(am^{(0)}_{\mathrm{pole},c})^{(n-4)}} + \mathcal{O}((am_c)^m). \tag{6}$$

In the HISQ formalism, this mass is related to the mass m_{0c} that appears in the action by [14]

$$m^{(0)}_{\mathrm{pole},c} = m_{0c}\left(1 - \frac{3(am_{0c})^4}{80} + \frac{23(am_{0c})^6}{2240} + \frac{1783(am_{0c})^8}{537\,600} - \frac{76\,943(am_{0c})^{10}}{23\,654\,400} + \cdots\right). \tag{7}$$

Introducing $G_n^{(0)}$ removes the explicit factors of the lattice spacing in the denominator of Eq. (4), and also cancels finite-a errors to all orders in a and zeroth order in α_s. Thus we expect finite-a errors that are reduced by a factor of order $\alpha_s(1/a) \approx 1/3$ when we divide G_n by the corresponding lowest-order lattice moment; and we find in practice that they are 3–4 times smaller.

A second modification is to replace the pole mass in $G_n/G_n^{(0)}$ by the value of the η_c mass obtained from the simulation, am_{η_c} (in lattice units) [22]:

$$\frac{G_n}{G_n^{(0)}}\left(\frac{am_{\eta_c}}{2am^{(0)}_{\mathrm{pole},c}}\right)^{n-4} = \frac{g_n}{g_n^{(0)}}\left(\frac{m_{\eta_c}}{2m_c(\mu)}\right)^{n-4} \tag{8}$$

up to $\mathcal{O}((am_c)^m\alpha_s)$ corrections. With this additional factor, the leading dependence on $m_c(\mu)$ enters through the ratio $m_c(\mu)/m_{\eta_c}$. Consequently small errors in the simulation parameter am_{0c} are mostly cancelled in this expression by corresponding shifts in the simulation value for am_{η_c}. This cancellation is accurate up to binding corrections of order $(v_c/c)^2 \approx 1/3$ in m_{η_c}, and therefore the impact of any tuning error in m_{0c} is 3 times smaller with this modification [23].

Combining these two modifications, we replace G_n by a reduced moment

$$R_n \equiv \begin{cases} G_4/G_4^{(0)} & \text{for } n = 4, \\ \dfrac{am_{\eta_c}}{2am^{(0)}_{\mathrm{pole},c}}(G_n/G_n^{(0)})^{1/(n-4)} & \text{for } n \geq 6. \end{cases} \tag{9}$$

The reduced moments can again be written in terms of continuum quantities:

$$R_n \equiv \begin{cases} r_4(\alpha_{\overline{\mathrm{MS}}}, \mu/m_c) & \text{for } n = 4, \\ \dfrac{r_n(\alpha_{\overline{\mathrm{MS}}}, \mu/m_c)}{2m_c(\mu)/m_{\eta_c}} & \text{for } n \geq 6, \end{cases} \tag{10}$$

up to $\mathcal{O}((am_c)^m\alpha_s)$ corrections, where r_n is obtained from g_n and its value, $g_n^{(0)}$, in lowest-order continuum perturbation theory:

$$r_n = \begin{cases} g_4/g_4^{(0)} & \text{for } n = 4, \\ (g_n/g_n^{(0)})^{1/(n-4)} & \text{for } n \geq 6. \end{cases} \tag{11}$$

The c mass is obtained from Eq. (10) with $n \geq 6$ using the nonperturbative lattice QCD (LQCD) value for R_n, the perturbative QCD (PQCD) estimate for r_n, and the experimental value for m_{η_c}, 2.980 GeV:

$$m_c(\mu) = \frac{m^{\mathrm{exp}}_{\eta_c}}{2}\frac{r_n^{\mathrm{PQCD}}}{R_n^{\mathrm{LQCD}}}. \tag{12}$$

Reduced moment R_4 is dimensionless and so depends only weakly on m_c. Simulation values for this moment can be compared with perturbation theory to obtain estimates for the QCD coupling: given the c-quark mass and a nonperturbative lattice QCD value for R_4, we solve the equation

$$R_4^{\mathrm{LQCD}} = r_4(\alpha_{\overline{\mathrm{MS}}}, \mu/m_c) \tag{13}$$

for $\alpha_{\overline{\mathrm{MS}}}(\mu)$. Ratios of reduced moments, like R_n/R_{n+2} for $n \geq 6$, can also be used in this way to estimate the coupling.

B. Simulation results

Our simulation results for $R_n(a, m_{u/d}, m_s)$ are listed for different moments n, lattice spacings a, and sea-quark masses in Table II; we also list ratios of reduced moments, R_n/R_{n+2} for $n \geq 6$. Some of these results are plotted versus the lattice spacing in Fig. 1. Our simulations did not include c-quark vacuum polarization, but the correction to the moments can be computed using perturbation theory (since c quarks are relatively heavy) [24]. We find that these corrections add 0.7% to R_4, and are of order 0.1% or less for the higher moments considered here. The R_n's in the table are corrected to include this effect.

The uncertainty quoted for each $R_n(a, m_{u/d}, m_s)$ with $n \geq 6$ is dominated by the uncertainty in our tuning of m_{0c} (other sources, such as statistical or finite-volume errors [25], are negligible). We tune the bare c-quark mass so that

TABLE II. Simulation results for $R_n(a, m_{u/d}, m_s)$ for different lattice parameter sets (see Table I). The inverse lattice spacing a^{-1} is in GeV. Extrapolations to zero lattice spacing and zero sea-quark masses are given for each quantity, together with the corresponding value for $m_c(\mu)$ (in GeV) or $\alpha_{\overline{\rm MS}}(\mu)$ for $n_f = 4$ flavors and $\mu = 3$ GeV.

Set:	1	2	3	4	5	6	7	8		
a^{-1}:	1.31	1.31	1.62	1.60	1.63	2.26	2.28	3.24	$a, m_{u/d/s} \to 0$	$m_c(\mu)$
R_6	1.448(3)	1.447(3)	1.494(3)	1.492(3)	1.491(3)	1.514(3)	1.511(3)	1.519(3)	1.528(11)	0.986(10)
R_8	1.372(3)	1.371(3)	1.387(3)	1.386(3)	1.384(3)	1.374(3)	1.373(3)	1.370(3)	1.370(10)	0.986(11)
R_{10}	1.329(3)	1.328(3)	1.326(3)	1.326(3)	1.324(3)	1.306(3)	1.305(3)	1.304(3)	1.304(9)	0.973(19)
R_{12}	1.294(3)	1.293(3)	1.284(3)	1.284(3)	1.281(3)	1.263(3)	1.262(3)	1.262(3)	1.265(9)	0.969(23)
R_{14}	1.264(3)	1.264(3)	1.252(2)	1.251(2)	1.248(2)	1.232(2)	1.231(2)	1.232(2)	1.237(9)	0.967(28)
R_{16}	1.239(2)	1.239(2)	1.228(2)	1.226(2)	1.223(2)	1.207(2)	1.206(2)	1.210(2)	1.215(9)	0.965(33)
R_{18}	1.218(2)	1.218(2)	1.208(2)	1.205(2)	1.202(2)	1.187(2)	1.187(2)	1.191(2)	1.198(9)	0.963(38)

Set:	1	2	3	4	5	6	7	8		
a^{-1}:	1.31	1.31	1.62	1.60	1.63	2.26	2.28	3.24	$a, m_{u/d/s} \to 0$	$\alpha_{\overline{\rm MS}}(\mu)$
R_4	1.162(1)	1.161(1)	1.189(1)	1.187(1)	1.187(1)	1.223(1)	1.221(1)	1.249(1)	1.281(5)	0.252(6)
R_6/R_8	1.055(1)	1.055(1)	1.078(1)	1.076(1)	1.077(1)	1.101(1)	1.101(1)	1.109(1)	1.113(2)	0.249(6)
R_8/R_{10}	1.033(1)	1.033(1)	1.046(1)	1.045(1)	1.046(1)	1.052(1)	1.052(1)	1.051(1)	1.049(2)	0.224(31)
R_{10}/R_{12}	1.027(1)	1.027(1)	1.033(1)	1.033(1)	1.034(1)	1.034(1)	1.034(1)	1.033(1)	1.031(2)	0.241(30)
R_{12}/R_{14}	1.023(1)	1.023(1)	1.025(1)	1.026(1)	1.026(1)	1.025(1)	1.025(1)	1.024(1)	1.022(2)	0.243(47)
R_{14}/R_{16}	1.020(1)	1.020(1)	1.020(1)	1.021(1)	1.021(1)	1.020(1)	1.020(1)	1.019(1)	1.017(2)	0.242(70)
R_{16}/R_{18}	1.017(1)	1.017(1)	1.016(1)	1.017(1)	1.017(1)	1.017(1)	1.017(1)	1.016(1)	1.014(2)	0.241(96)

our simulations give correct masses for the η_c [26]. Our tuning is limited by the precision with which we know the lattice spacing a for any given parameter set in Table I, since simulations give masses in lattice units (that is, am_{η_c}). We determine lattice spacings by combining MILC's values for r_1/a (see Table I), which are accurate to around 0.6%, with a value for r_1 determined from the upsilon spectrum: $r_1 = 0.321(5)$ fm [16], which is accurate to 1.5%. The corresponding uncertainties in the R_n's are 3 times smaller, because of the reduced sensitivity of m_c/m_{η_c} (see above). We include the uncertainty due to r_1/a (0.6%/3 = 0.2%) in the uncertainties reported for each separate $R_n(a)$ in Table II. The uncertainty due to r_1 (1.5%/3 = 0.5%) is included only in our final results, after extrapolation (since changes in r_1 affect all $R_n(a)$'s by the same amount).

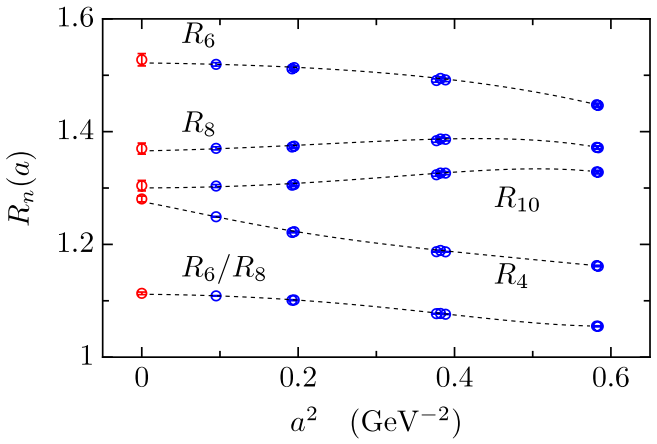

FIG. 1 (color online). Reduced moments R_n and a ratio of these moments from lattice simulations with different lattice spacings a. The tight clusters of points at each of the three largest lattice spacings correspond to results for different sea-quark masses. The dashed lines show the functions used to fit the lattice results, with the sea-quark masses set equal to the masses used at the smallest lattice spacing. These extrapolation functions were used to obtain the $a = 0$, $m_{u/d/s} = 0$ results shown in the plot.

Reduced moment R_4 and our ratios of reduced moments are much less sensitive to errors in m_{0c} because the c mass enters only through radiative corrections, in perturbation theory. Consequently uncertainties due to mistunings of m_{0c} are smaller by an order of magnitude or more for these quantities. We account for potential tuning errors by assigning an uncertainty of 0.05% to each of the R_4's and ratios.

We also include in Table II our results extrapolated to zero lattice spacing and zero sea-quark mass [27]. Our extrapolation procedure is described in the next section.

C. am_c, m_q/m_c Extrapolations

Table II and Fig. 1 show that our reduced moments depend only weakly on the lattice spacing, with most moments changing by 0.5% or less between our two smallest lattice spacings and only a few percent over our entire range. The dependence on the sea-quark masses is even weaker. We nevertheless correct our results by fitting the variation over our different sets of lattice parameters (Table I) and extrapolating to zero lattice spacing and zero sea-quark mass. We do this with a constrained fit

[28,29] of our simulation data to a function of the form

$$R_n(a) = R_n(0)(1 + c_{n,2}(am_c)^2\alpha_s + c_{n,4}(am_c)^4\alpha_s + c_{n,6}(am_c)^6\alpha_s + c_{n,8}(am_c)^8\alpha_s + \cdots) \times (1 + f_{n,1}(2m_{u/d} + m_s)/m_c + \cdots) \quad (14)$$

where we take $m_c = 1$ GeV and $\alpha_s = \alpha_s(1/a)$. This form is motivated by the pattern of a^n errors in our lattice actions, and by chiral perturbation theory, which implies nonperturbative corrections that depend linearly on the sea-quark masses. (There is sea-quark mass dependence in perturbation theory, as well, but it enters at $\mathcal{O}(\alpha_s^2(m_q/m_c)^2)$ and is negligible here.)

The extrapolated results are largely independent of the exact functional form used for the extrapolation provided reasonable Bayesian priors are included (in the χ^2 function that is minimized in the fit) for each of the coefficients $c_{n,i}$ and $f_{n,i}$ [28,29]. We use the same Gaussian prior, centered at zero with width $\sigma_c = 1$, for every $c_{n,i}$, for all moments and moment ratios except R_4. Moment R_4 has larger a^2 errors and needs a wider prior; we take $\sigma_c = 5$. We use a prior with width $\sigma_f = 0.1$ for the $f_{n,i}$, which is twice as large as the largest coefficient obtained from the fits.

The error estimates from our fits initially increase, and χ^2 decreases, as we add successively higher-order terms in the $(am_c)^2$ and m_q/m_c expansions. Eventually the errors stop increasing and χ^2 stops changing, again assuming proper priors for all fit parameters. It is important to add terms through this point in order to avoid underestimating uncertainties in the final fit results. Adding further terms has no effect on fit results (values or errors).

Only a single term is needed in each series to get good fits for R_n with $n \geq 6$ if we discard data from the largest lattice spacing; and our final results (values and errors) are little changed. We, however, retain results from the coarsest lattices, despite the large value of am_c for those lattices, in order to test our priors. Fitting all of our simulation data, we get good fits with two terms in the $(am_c)^2$ and a single term in the m_q/m_c expansion. To be certain of convergence, we used eight terms in the first expansion and two in the second to obtain the extrapolated results in Table II. The fact that we get good fits (χ^2 per data point less than one) even when we include data from the coarsest lattices helps validate the design of our fit function and priors, and it reassures us that our fits are not underestimating errors.

Moment R_4 and the ratios of moments are more accurately determined in our simulation than the other R_n's, and so typically require an additional term in the $(am_c)^2$ expansion. Again, however, the eight terms we use are many more than the minimum needed.

Our final error estimates depend upon the widths of our priors [29]. We tested these widths in a couple of ways, beyond including simulation data from the coarsest lattices. First we compared our widths with the values suggested by the empirical Bayes procedure described in [28]. This procedure uses the variation in the data itself to determine, for example, an optimal value for σ_c. The widths we use are 2 to 4 times larger than what is indicated by the empirical Bayes criterion, suggesting that our error estimates are conservative. The dominant fit coefficients in the $(am_c)^2$ expansion for R_6, for example, range between -0.05 and -0.20, which is much smaller than the $\sigma_c = 1$ we use.

As a second test, we verified that our extrapolation procedure gives consistent results when data from either the smallest or the largest lattice spacing is discarded. That is, we demonstrated that results obtained from the truncated data sets agree within errors with results from the full set of simulation data. This shows that our error estimates are robust even when working with limited simulation data sets. As mentioned above, our final results are not much affected by data from the coarsest lattice spacing. Simulation data from the finest lattice spacing, on the other hand, has a very significant impact.

IV. EXTRACTING $m_c(\mu)$ AND $\alpha_{\overline{\rm MS}}(\mu)$

To convert the extrapolated reduced moments into c masses and coupling constants, we require perturbative expansions for the r_n in Eq. (12). These are easily computed from the expansions for g_n [3–9] using Eq. (11); details can be found in the Appendix. The perturbative expansions have the form

$$r_n = 1 + r_{n,1}\alpha_{\overline{\rm MS}}(\mu) + r_{n,2}\alpha^2_{\overline{\rm MS}}(\mu) + r_{n,3}\alpha^3_{\overline{\rm MS}}(\mu) + \ldots \quad (15)$$

where we set the renormalization scale μ to 3 GeV [30]. The full third-order coefficients for the $n = 4, 6, 8$ moments were computed for this analysis and are presented in the Appendix. The third-order coefficients for moments with $n \geq 10$ are only partially complete: our analysis includes all μ-dependent terms (that is, $\log^n(\mu/m_c)$ terms), but the constant parts have not yet been computed. Consequently we take the truncation uncertainty in r_n to be of order [31]

$$\sigma_{r_n} = \begin{cases} r_n^{\max}\alpha^4_{\overline{\rm MS}}(\mu) & \text{for } n = 4, 6, 8, \\ r_n^{\max}\alpha^3_{\overline{\rm MS}}(\mu) & \text{for } n \geq 10, \end{cases} \quad (16)$$

where

$$r_n^{\max} = \max(|r_{n,1}|, |r_{n,2}|, |r_{n,3}|). \quad (17)$$

Another source of uncertainty in all of our moments comes from nonperturbative effects. In the previous section, we discuss how we remove nonperturbative contributions involving the sea-quark masses. To assess the importance of gluonic contributions, we also include the leading gluon-condensate contribution in our moments [2,32,33]. We do this by multiplying r_n by a factor of the

form $(1 + d_n\langle\alpha_s G^2/\pi\rangle/(2m_c)^4))$ where, here, $m_c = m_c(m_c)$ and d_n is computed through leading order in $\alpha_{\overline{\rm MS}}(m_c)$. The value of the condensate is not well-known; we set $\langle\alpha_s G^2/\pi\rangle = 0 \pm 0.012$ GeV^4, which covers the range of most current estimates [34].

Note that coefficients in the r_n expansion, Eq. (15), depend upon $m_c(\mu)$ through scale-dependent logarithms, $\log^n(\mu/m_c(\mu))$. Consequently, the mass appears on both sides of Eq. (12), and the equation is an implicit equation for $m_c(\mu)$. The $m_c(\mu)$ dependence on the right-hand side, however, is suppressed by $\alpha_{\overline{\rm MS}}(\mu)$, and therefore the equation is easily solved numerically.

Our final results for the c-quark's mass, $m_c(\mu)$ at $\mu = 3$ GeV for $n_f = 4$ flavors in the $\overline{\rm MS}$ scheme, are listed in Table II, and plotted in the upper-left panel of Fig. 2. As is clear from the figure, all moments agree on the mass although the higher moments may be less trustworthy (see [2]). The first two moments ($n = 6, 8$) give results that are twice as accurate as the others because we have full $\mathcal{O}(\alpha^3_{\overline{\rm MS}})$ perturbation theory in these cases. We average the two results, which agree, to obtain our final result for the mass

$$m_c(3\ \text{GeV}, n_f = 4) = 0.986(10)\ \text{GeV}. \tag{18}$$

Evolving down to scale $\mu = m_c(\mu)$ using fourth-order evolution [35–38], this is equivalent to [39]

$$m_c(m_c, n_f = 4) = 1.268(9)\ \text{GeV}. \tag{19}$$

We used $\alpha_{\overline{\rm MS}}(3\ \text{GeV}, n_f = 4) = 0.252(10)$ in the perturbation theory needed to extract $m_c(\mu)$. We derived this from the current Particle Data Group average for the $n_f = 5$ coupling at $\mu = M_Z$, which is 0.1176(20) [40]. The coupling can also be extracted directly from R_4 and from the ratios R_n/R_{n+2}, as discussed above. Taking $m_c(\mu) = 0.986(10)$ GeV, we obtain the couplings, for scale $\mu = 3$ GeV and $n_f = 4$, shown in Table II. The first two determinations listed in the table are far more accurate than the others because we know perturbation theory through third order. We can average these to obtain a composite value for the coupling of

$$\alpha_{\overline{\rm MS}}(3\ \text{GeV}, n_f = 4) = 0.251(6). \tag{20}$$

To allow comparison with other work we converted our couplings to $n_f = 5$ by adding a b quark with mass $m_b(m_b) = 4.20(7)$ GeV [40], and evolving them to scale M_Z. The results are shown in Fig. 3. Averaging the first two numbers, which agree with each other, we get

$$\alpha_{\overline{\rm MS}}(M_Z, n_f = 5) = 0.1174(12). \tag{21}$$

The leading sources of uncertainty in $m_c(\mu)$ and $\alpha_{\overline{\rm MS}}(M_Z)$ are listed in Table III for those calculations where we have full perturbation theory through $\mathcal{O}(\alpha^3_{\overline{\rm MS}})$ [29]. The dominant uncertainty in the masses comes from potential tuning errors in the c-quark masses used in the simulation. Truncation errors from perturbation theory dominate for the coupling, with nonperturbative contributions from the gluon condensate also become important. In addition to the various sources discussed above, there are also uncertainties due to the finite spatial volume of our lattices; our lattices were approximately 2.5 fm across. While our simulations showed no measurable volume dependence [25], lattice perturbation theory shows finite-volume sensitivity for the higher (more infrared) moments. This is negligible for lower moments but grows with n. The

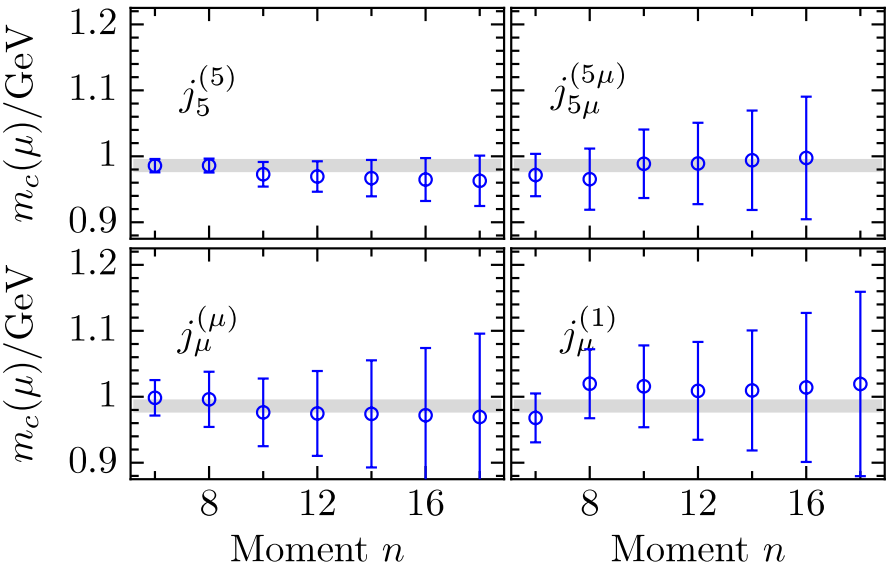

FIG. 2 (color online). $m_c(\mu)$, for $\mu = 3$ GeV and $n_f = 4$ flavors, from different moments of correlators built from four different lattice operators. The gray band is our final result for the mass, 0.986(10) GeV, which comes from the first two moments of the pseudoscalar correlator (upper-left panel).

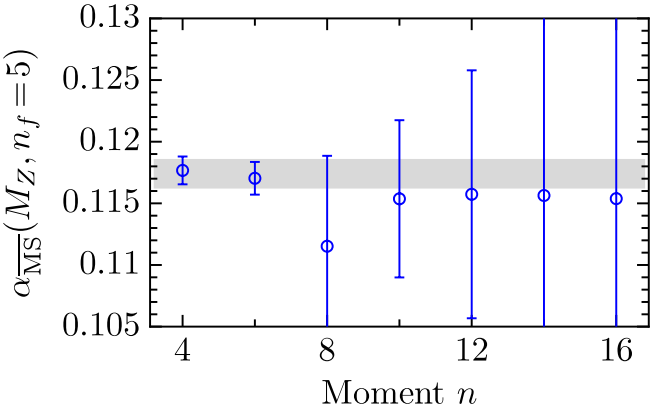

FIG. 3 (color online). $\alpha_{\overline{\rm MS}}(M_Z, n_f = 5)$ from R_4 and ratios R_n/R_{n+2}. The gray band is our final result for the coupling, 0.1174(12), which comes from R_4 and R_6/R_8.

finite-volume sensitivity is mostly an artifact of perturbation theory; confinement significantly reduces finite-volume effects. Consequently we assign a finite-volume error to our perturbative factors that is equal to the entire finite-volume correction in perturbation theory.

V. $m_c(\mu)$ FROM OTHER CORRELATORS

The close agreement on m_c between different moments is important evidence that we understand our systematic errors since these enter quite differently in different moments. To further check this we repeated our analysis for three different correlators, which we formed by replacing the pseudoscalar operator $m_{0c} j_5$ with each of the following c-quark currents on the lattice:

$$j_\mu^{(1)} \equiv \bar{\psi}_c(x + a\hat{\mu})\gamma_\mu \psi_c(x), \tag{22}$$

TABLE III. Sources of uncertainty in the determinations of $m_c(\mu = 3\ \text{GeV}, n_f = 4)$ and $\alpha_{\overline{\rm MS}}(M_Z, n_f = 5)$ from different reduced moments R_n of the pseudoscalar correlator. The uncertainties listed are percentages of the final results.

	$m_c(\mu)$		$\alpha_{\overline{\rm MS}}(M_Z)$	
	R_6	R_8	R_4	R_6/R_8
a^2 extrapolation	0.2%	0.3%	0.4%	0.2%
Perturbation theory	0.4%	0.3%	0.6%	0.6%
$\alpha_{\overline{\rm MS}}$ uncertainty	0.3%	0.4%	...	...
$m_c(\mu)$ uncertainty	...	...	0.1%	0.1%
Gluon condensate	0.3%	0.0%	0.4%	0.7%
Statistical errors	0.1%	0.0%	0.2%	0.1%
m_{0c} errors from r_1/a	0.5%	0.6%	0.3%	0.4%
m_{0c} errors from r_1	0.6%	0.6%	0.1%	0.1%
$m_{u/d/s}$ extrapolation	0.2%	0.2%	0.2%	0.4%
Finite volume	0.1%	0.1%	0.0%	0.3%
$\mu \to M_Z$ evolution	0.0%	0.0%	0.1%	0.1%
Total	1.0%	1.1%	1.0%	1.1%

$$j_\mu^{(\mu)} \equiv \bar{\psi}_c(x)\gamma_\mu \psi_c(x), \tag{23}$$

$$j_{5\mu}^{(5\mu)} \equiv \bar{\psi}_c(x)\gamma_5\gamma_\mu \psi_c(x). \tag{24}$$

The first two currents are different lattice discretizations of the vector current and were evaluated for spacelike μ's; and the first of these was evaluated in Coulomb gauge. The third current is a lattice discretization of the axial vector current and was evaluated for timelike μ. The superscript on each j labels the "taste" carried by that operator, using the notation presented in the Appendices of [14]. Taste is a spurious quantum number, analogous to flavor, that is an artifact of staggered-quark lattice discretizations like the HISQ formalism. Taste should not affect physical results and therefore operators carrying different taste here should give identical results in the $a \to 0$ limit. By studying these different currents, we not only test for conventional systematic errors, but also verify that HISQ-specific taste effects are negligible [41].

A complication in our lattice analysis of these vector (or axial-vector) correlators is that none of the currents is conserved (or partially conserved) on the lattice. Consequently, each lattice current is related to its corresponding continuum operator by a renormalization constant:

$$j_{\rm cont} = Z^{(j)} j + \mathcal{O}(a^2) \qquad Z^{(j)} \equiv Z^{(j)}(\alpha_{\overline{\rm MS}}(\pi/a), am_{0c}) \tag{25}$$

where j is one of the lattice currents $j_\mu^{(1)}$, $j_\mu^{(\mu)}$, or $j_{5\mu}^{(5\mu)}$, and $j_{\rm cont}$ is the continuum current $j_\mu = \bar{\psi}\gamma_\mu\psi$ for the first two j's and $j_{5\mu} = \bar{\psi}\gamma_5\gamma_\mu\psi$ for the last. Consequently moments of the correlators of these lattice currents have the form

$$G_n^{(j)} = \frac{1}{Z^{(j)^2}} \frac{g_n^{(j_{\rm cont})}(\alpha_{\overline{\rm MS}}(\mu), \mu/m_c)}{(am_c(\mu))^{n-2}}, \tag{26}$$

where $Z^{(j)^2} G_n^{(j)}$ is the continuum result for $n \geq 4$. To cancel the renormalization factor we redefine the reduced moments for these correlators to be

$$R_n^{(j)} \equiv \frac{am^{(j)}}{2am_{0c}} \left(\frac{G_n^{(j)}}{G_{n-2}^{(j)}} \frac{G_{n-2}^{(j0)}}{G_n^{(j0)}} \right)^{1/2} \tag{27}$$

$$\equiv \frac{r_n^{(j_{\rm cont})}(\alpha_{\overline{\rm MS}}, \mu/m_c)}{2m_c(\mu)/m^{(j)}} \tag{28}$$

where $n \geq 6$, and $m^{(j)}$ is the ψ mass for the vector currents (which couple to the ψ) and the η_c mass for the axial-vector current. Again we divide each moment $G_n^{(j)}$ by its value $G_n^{(j0)}$ in leading-order lattice perturbation theory in order to minimize finite-lattice-spacing errors. And again the perturbative expansion for $r_n^{(j_{\rm cont})}$ can be obtained from

TABLE IV. Simulation results for the reduced moments $R_n^{(j)}$, extrapolated to $a = 0$, from correlators of local axial-vector and vector lattice currents, and a point-split lattice vector current. Corresponding values for $m_c(\mu)$ (in GeV), for $\mu = 3$ GeV and $n_f = 4$, are also given. Only results for parameter sets 1, 4, and 6 from Table I were used for the first and last currents; results from these sets were combined with results from set 8 (the smallest lattice spacing) for $j_\mu^{(\mu)}$.

	$j_{5\mu}^{(5\mu)}$		$j_\mu^{(\mu)}$		$j_\mu^{(1)}$	
n	$R_n^{(j)}$	$m_c(\mu)$	$R_n^{(j)}$	$m_c(\mu)$	$R_n^{(j)}$	$m_c(\mu)$
6	1.240(27)	0.97(3)	1.233(16)	1.00(3)	1.261(30)	0.97(4)
8	1.159(25)	0.97(5)	1.183(15)	1.00(4)	1.163(27)	1.02(5)
10	1.126(24)	0.99(5)	1.162(15)	0.98(5)	1.132(27)	1.02(6)
12	1.103(24)	0.99(6)	1.139(15)	0.97(6)	1.113(26)	1.01(7)
14	1.082(23)	0.99(8)	1.120(15)	0.97(8)	1.094(26)	1.01(9)
16	1.064(23)	1.00(9)	1.106(14)	0.97(10)	1.076(25)	1.01(11)
18			1.093(14)	0.97(13)	1.059(25)	1.02(14)

continuum perturbation theory expansions for the $g_n^{(j_{\rm cont})}$ (see the Appendix).

Our simulation results for $R_n^{(j)}$, extrapolated to lattice spacing $a = 0$, are given in Table IV for different moments n and each of the three currents [42]. Perturbative coefficients for the vector-current $r_n^{(j_{\rm cont})}$'s are discussed in the Appendix; the coefficients for the temporal axial-vector current can be derived from the pseudoscalar coefficients (also in the Appendix) using Ward identities [43].

By combining perturbative with nonperturbative results, we obtain the values for $m_c(\mu)$, with $\mu = 3$ GeV and $n_f = 4$, that are listed in Table IV and plotted in the top-right and bottom panels of Fig. 2. Results from all moments agree with each other and with the pseudoscalar result (the gray band in the plots), although here the errors are about twice as large for the smaller moments.

Values for the lowest four moments of the vector correlator are derived from experimental data for e^+e^- annihilation in [2]. Converting these into reduced moments, we compare them with our extrapolated $R_n^{(j)}$'s for $j = j_\mu^{(\mu)}$ (from Table IV) in Fig. 4. We find that experiment and our simulation results agree to within combined errors of better than 2%. This comparison is more accurate than comparing masses, because we are comparing the (reduced) moments directly, without recourse to further perturbation theory.

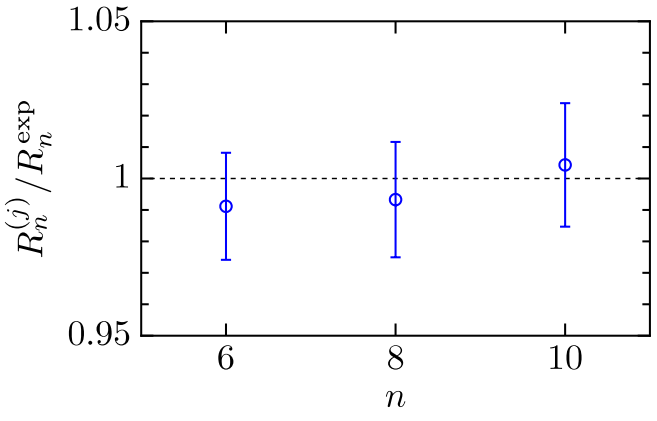

FIG. 4 (color online). Ratio of the extrapolated simulation results from Table IV for $R_n^{(j)}$, with $j = j_\mu^{(\mu)}$, to results derived from experiment in [2] for different moments n.

VI. CONCLUSIONS

Our results are by far the most accurate determination of the c-quark mass from lattice QCD [44]. Such precision is possible because the matching between lattice parameters and continuum parameters here relies upon continuum perturbation theory, which is much simpler than lattice QCD perturbation theory. Consequently perturbation theory can be pushed to much higher orders. The precision of this continuum calculation is matched by that of our nonperturbative lattice analysis because of the quality of the MILC configurations and of our highly corrected HISQ action for c quarks.

The agreement between masses from different moments, and from different correlators—27 determinations in all—is an important check on systematic errors of all sorts since these enter in very different ways in each calculation. Note that the different reduced moments in our analysis vary in value by as much as 43% (from 1.06 to 1.52), and yet they all agree on the value of m_c to within a few percent once we account for differences in the perturbative parts.

One surprising feature of our results is that even the higher moments give correct values for the quark mass, albeit with larger errors. Nonperturbative effects grow with n but our results show no systematic deviation until very large n, as is evident in Fig. 5 which shows results for $20 \leq n \leq 62$. We have not included potential errors due to the gluon condensate in this figure. The error bars would have been much larger had we done so. For example, they would have been about 5 times larger at $n = 40$ in the pseudoscalar plot (16% rather than 3%). This might suggest that the condensate is smaller than we allowed for—say

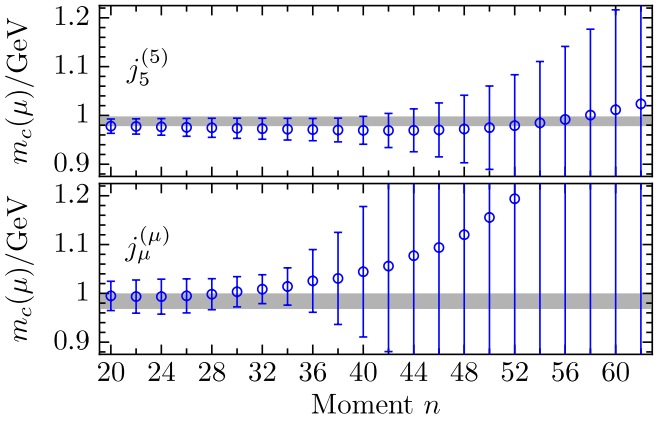

FIG. 5 (color online). $m_c(\mu = 3\ \text{GeV})$ from large-n moments of the pseudoscalar and the (local) vector correlators. The gray band is our final result for the mass (from $n = 6, 8$), 0.986 (10) GeV. The perturbative part of the analysis was evaluated at $\mu = m_c(\mu)$ using formulas from [7], and the results evolved to $\mu = 3$ GeV using fourth-order evolution. Uncertainties due to the gluon condensate are not included (see text).

$\langle \alpha_s G^2/\pi \rangle \leq 0.003\ \text{GeV}^4$—but we have not analyzed this carefully enough to make a strong statement. The error bars shown in the plots start to grow rapidly just where it becomes clear that perturbation theory is failing (because of large coefficients).

Our lattice result for the mass, $m_c(3\ \text{GeV}, n_f = 4) = 0.986(10)$ GeV, agrees well with the continuum determination from e^+e^- annihilation data, which gives 0.986 (13) GeV [2]. This provides further strong evidence that the different systematic errors in each calculation are understood. Similarly our new value for the coupling, $\alpha_{\overline{\text{MS}}}(M_Z, n_f = 5) = 0.1174(12)$, agrees very well with nonlattice determinations [40,45] and our other determinations from lattice QCD [13,29]. It is also more accurate than most determinations.

The close agreement of our results with nonlattice determinations of the mass and coupling, and the taste independence of our masses, is also further evidence that the simulation methods we use are valid. While early concerns about the light-quark discretization used here have been largely addressed [46,47], it remains important to test the simulation technology of lattice QCD at increasing levels of precision, given the critical importance of lattice results for phenomenology.

Our results are particularly relevant to the recent, very accurate analysis of π, K, D, and D_s meson decay constants using the same HISQ formalism for valence quarks and many of the same MILC configuration sets that we use here [15]. The correlators in our pseudoscalar analysis are identical to those used to extract the decay constants in the earlier study, except that here the light valence quarks have been replaced by c quarks, which should make finite-a errors worse. The agreement of our pseudoscalar analysis of R_6 with the continuum analysis for $m_c(\mu)$ indicates that our extrapolated lattice $c\bar{c}$ correlators are reliable to within 2% or better. The accuracy of our $c\bar{c}$ results, together with the demonstrated accuracy of the π and K results in [15] from light-quark correlators, strongly suggest that the corresponding D and D_s predictions, from correlators with a light quark and a c quark, are reliable. This conclusion is made more important by the 3.6σ discrepancy between the D_s prediction and recent experimental results [48–50].

The lattice analysis will be improved as data becomes available for smaller lattice spacings. Also a very accurate c-quark mass will allow us to make similarly accurate determinations of the s-quark mass [51]. This is because the ratio m_s/m_c can be determined very accurately in lattice simulations where the s and c quarks are analyzed using the same formalism, as here. Finally four-loop perturbation theory for additional moments would improve both lattice and continuum determinations.

ACKNOWLEDGMENTS

We would like to thank A. Maier, P. Maierhöfer, and P. Marquard for providing $\bar{C}_3^{(30)}$ for the pseudoscalar correlator prior to publication. We are grateful to the MILC Collaboration for the use of their gluon configurations. We thank Rainer Sommer for useful discussions. The lattice QCD computing was done on UKQCD's QCDOCX cluster, USQCD's Fermilab cluster, and at the Ohio Supercomputer Center. The work was supported by grants from: the Deutsche Forschungsgemeinschaft, SFB-Transregio 9; the Department of Energy [DE-FG02-91-ER40690, DE-AC02-98CH10886(BNL)]; the Leverhulme Trust; the Natural Sciences and Engineering Research Council; the National Science Foundation; and the Science and Technology Facilities Council.

APPENDIX A: CONTINUUM PERTURBATION THEORY

The correlators of two pseudoscalar ($\imath\bar{\psi}_c\gamma_5\psi_c$), vector ($\bar{\psi}_c\gamma_\mu\psi_c$), and axial-vector ($\bar{\psi}_c\gamma_\mu\gamma_5\psi_c$) currents are defined by

$$q^2\Pi^p(q^2) = i\int dx e^{iqx}\langle 0|Tj_5(x)j_5(0)|0\rangle, \tag{A1}$$

$$(q_\mu q_\nu - q^2 g_{\mu\nu})\Pi^\delta(q^2) + q_\mu q_\nu \Pi_L^\delta(q^2) = \Pi_{\mu\nu}^\delta(q) = i\int dx e^{iqx}\langle 0|Tj_\mu^\delta(x)j_\nu^\delta(0)|0\rangle, \tag{A2}$$

where $\delta = v$ and a for the vector and axial-vector cases, respectively. The polarization functions can be expanded in the variable $z = q^2/(2m_c(\mu))^2$:

$$\bar{\Pi}^\delta(q^2) = \frac{3}{16\pi^2}\sum_{k=-1}^{\infty}\bar{C}_k^\delta z^k. \tag{A3}$$

TABLE V. Moments of the pseudoscalar (upper eight lines) and the vector (lower eight lines) correlators, where currently unknown coefficients are denoted by center dots and set to zero in our analysis. The numbers correspond to QCD with one massive c quark and three massless (u, d, s) quarks.

k	$\bar{C}_k^{(0)}$	$\bar{C}_k^{(10)}$	$\bar{C}_k^{(11)}$	$\bar{C}_k^{(20)}$	$\bar{C}_k^{(21)}$	$\bar{C}_k^{(22)}$	$\bar{C}_k^{(30)}$	$\bar{C}_k^{(31)}$	$\bar{C}_k^{(32)}$	$\bar{C}_k^{(33)}$
1	1.3333	3.1111	0.0000	0.1154	−6.4815	0.0000	−1.2224	2.5008	13.5031	0.0000
2	0.5333	2.0642	1.0667	7.2362	1.5909	−0.0444	7.0659	−7.5852	0.5505	0.0321
3	0.3048	1.2117	1.2190	5.9992	4.3373	1.1683	14.5789	7.3626	4.2523	−0.0649
4	0.2032	0.7128	1.2190	4.2670	4.8064	2.3873	⋯	14.7645	11.0345	1.4589
5	0.1478	0.4013	1.1821	2.9149	4.3282	3.4971	⋯	16.0798	16.6772	4.4685
6	0.1137	0.1944	1.1366	1.9656	3.4173	4.4992	⋯	14.1098	19.9049	8.7485
7	0.0909	0.0500	1.0912	1.3353	2.2995	5.4104	⋯	10.7755	20.3500	14.1272
8	0.0749	−0.0545	1.0484	0.9453	1.0837	6.2466	⋯	7.2863	17.9597	20.4750
1	1.0667	2.5547	2.1333	2.4967	3.3130	−0.0889	−5.6404	4.0669	0.9590	0.0642
2	0.4571	1.1096	1.8286	2.7770	5.1489	1.7524	−3.4937	6.7216	6.4916	−0.0974
3	0.2709	0.5194	1.6254	1.6388	4.7207	3.1831	⋯	7.5736	13.1654	1.9452
4	0.1847	0.2031	1.4776	0.7956	3.6440	4.3713	⋯	4.9487	17.4612	5.5856
5	0.1364	0.0106	1.3640	0.2781	2.3385	5.3990	⋯	0.9026	18.7458	10.4981
6	0.1061	−0.1158	1.2730	0.0070	0.9553	6.3121	⋯	−3.1990	16.9759	16.4817
7	0.0856	−0.2033	1.1982	−0.0860	−0.4423	7.1390	⋯	−6.5399	12.2613	23.4000
8	0.0709	−0.2660	1.1351	−0.0496	−1.8261	7.8984	⋯	−8.6310	4.7480	31.1546

The polarization function and the c-quark mass $m_c(\mu)$ are renormalized in the $\overline{\text{MS}}$ scheme.

The longitudinal part of the axial-vector current (which is of interest in the present context) and the pseudoscalar correlator are related by the axial Ward identity [52]

$$q^\mu q^\nu \Pi^a_{\mu\nu}(q) = (2m)^2 q^2 \Pi^p(q^2) + \text{contact term}. \quad \text{(A4)}$$

Comparing different orders in z,

$$\bar{C}^{\,p}_{k+1} = \bar{C}^a_{L,k}, \quad \text{for } k \geq -1, \quad \text{(A5)}$$

allows us to extract moments of the pseudoscalar correlator from those of the longitudinal part of the axial-vector correlator, and *vice versa*. The contact term contributes only to $k = -2$. The coefficients of the perturbative expansion depend logarithmically on m_c and can be written in the form

$$\begin{aligned}\bar{C}_k = {} & \bar{C}_k^{(0)} + \frac{\alpha_s(\mu)}{\pi}(\bar{C}_k^{(10)} + \bar{C}_k^{(11)} l_{m_c}) \\ & + \left(\frac{\alpha_s(\mu)}{\pi}\right)^2 (\bar{C}_k^{(20)} + \bar{C}_k^{(21)} l_{m_c} + \bar{C}_k^{(22)} l_{m_c}^2) \\ & + \left(\frac{\alpha_s(\mu)}{\pi}\right)^3 (\bar{C}_k^{(30)} + \bar{C}_k^{(31)} l_{m_c} + \bar{C}_k^{(32)} l_{m_c}^2 + \bar{C}_k^{(33)} l_{m_c}^3) \\ & + \ldots, \end{aligned} \quad \text{(A6)}$$

where $l_{m_c} \equiv \log(m_c^2(\mu)/\mu^2)$. The coefficients $\bar{C}_k^{(ij)}$ up through $k = 8$ are listed in Table V for both pseudoscalar and vector correlators.

The four-loop coefficients $\bar{C}_1^{(30)}$ and $\bar{C}_2^{(30)}$ for the pseudoscalar correlator are new [53]; and $\bar{C}_1^{(30)}$ for the vector correlator comes from [8,9]. The four-loop coefficients $\bar{C}_3^{(30)}$ for the pseudoscalar case is also new [10], as is $\bar{C}_2^{(30)}$ for the vector case [54]. The order α_s^2 terms up through $k = 8$ are given in [3–5], while results for higher k values are given in [6,7]. See also [55] for n_f-dependent four-loop terms, and [7] for the pseudoscalar case. Throughout this paper we take the number of light (massless) active quark flavors to be $n_l = 3$, and the number of heavy (massive) quarks is set to $n_h = 1$. For numerical work, we use $\mu = 3$ GeV.

The expansion coefficients $\bar{C}_k$ are related to the coefficients g_n of Eq. (4) by

$$\frac{g_{2k+2}}{g^{(0)}_{2k+2}} = \frac{\bar{C}_k}{\bar{C}_k^{(0)}}, \quad \text{(A7)}$$

and the coefficients $r_{n,i}$ in Eq. (15) are obtained through the series expansion of Eq. (11). For the vector correlator the coefficients $r^{(j_\mu)}_{n,i}$ are defined through the series expansions of

$$r^{(j_\mu)}_{2k+2} = \left(\frac{\bar{C}^v_k}{\bar{C}^{v,(0)}_k} \frac{\bar{C}^{v,(0)}_{k-1}}{\bar{C}^v_{k-1}}\right)^{1/2}. \quad \text{(A8)}$$

[1] J. H. Kuhn and M. Steinhauser, Nucl. Phys. **B619**, 588 (2001); **B640**, 415 (2002).

[2] J. H. Kuhn, M. Steinhauser, and C. Sturm, Nucl. Phys. **B778**, 192 (2007).

[3] K. G. Chetyrkin, J. H. Kuhn, and M. Steinhauser, Phys. Lett. B **371**, 93 (1996).

[4] K. G. Chetyrkin, J. H. Kuhn, and M. Steinhauser, Nucl. Phys. **B482**, 213 (1996).

[5] K. G. Chetyrkin, J. H. Kuhn, and M. Steinhauser, Nucl. Phys. **B505**, 40 (1997).

[6] R. Boughezal, M. Czakon, and T. Schutzmeier, Nucl. Phys. B, Proc. Suppl. **160**, 160 (2006).

[7] A. Maier, P. Maierhofer, and P. Marquard, Nucl. Phys. **B797**, 218 (2008).

[8] K. G. Chetyrkin, J. H. Kuhn, and C. Sturm, Eur. Phys. J. C **48**, 107 (2006).

[9] R. Boughezal, M. Czakon, and T. Schutzmeier, Phys. Rev. D **74**, 074006 (2006).

[10] The result for the third pseudoscalar moment, $\bar{C}_3^{30} = 14.5789$, was provided to us by A. Maier, P. Maierhöfer, and P. Marquard prior to publication.

[11] For an earlier exploratory analysis, using quenched ($n_f = 0$) QCD and less highly improved actions, see A. Bochkarev and P. de Forcrand, Nucl. Phys. **B477**, 489 (1996); Nucl. Phys. B, Proc. Suppl. **53**, 305 (1997); For a recent related analysis using light-quark correlators see: E. Shintani *et al.* (JLQCD Collaboration and TWQCD Collaboration), arXiv:0807.0556.

[12] C. T. H. Davies *et al.* (HPQCD Collaboration), Phys. Rev. Lett. **92**, 022001 (2004).

[13] Q. Mason *et al.* (HPQCD Collaboration), Phys. Rev. Lett. **95**, 052002 (2005).

[14] E. Follana *et al.* (HPQCD Collaboration), Phys. Rev. D **75**, 054502 (2007).

[15] E. Follana, C. T. H. Davies, G. P. Lepage, and J. Shigemitsu (HPQCD Collaboration), Phys. Rev. Lett. **100**, 062002 (2008).

[16] A. Gray, I. Allison, C. T. H. Davies, E. Dalgic, G. P. Lepage, J. Shigemitsu, and M. Wingate, Phys. Rev. D **72**, 094507 (2005); The error on the r_1 quoted in this paper, $r_1 = 0.321(5)$ fm, includes estimates of all errors involved in simulating the upsilons. This value has been extensively checked in many other calculations: see, for example, [12,15] for 11 other calculations that verify this value with precisions ranging from 1.5% to 3%.

[17] C. Aubin *et al.*, Phys. Rev. D **70**, 094505 (2004).

[18] The HISQ action, like all staggered-quark discretizations (but unlike many other discretizations), has an exact chiral symmetry in the limit of massless of quarks. The cutoff independence follows from the corresponding PCAC relationship.

[19] The value for t/a at the middle of the lattice was set to 0 in order to preserve the symmetry between t and $-t$. This choice causes odd moments to vanish, for example. The value chosen for this point does not matter in our analysis because contributions to our moments from this point are negligibly small (because of the exponential falloff in the correlators at large t).

[20] One might worry about large nonperturbative contributions to the η_c mass from $c\bar{c} \to$ gluons $\to c\bar{c}$ coming, for example, from mixing between the η_c and a nearby glueball. Such an effect is largely ruled out by the fact that our simulation (which does not allow such mixing) gives the correct masses for both the η_c and the ψ. In particular, the difference between their masses in the simulation agrees with experiments to within ± 5 MeV, which is less than 0.2% of the η_c's mass [14].

[21] The leading-order propagator $G^{(0)}(t)$ is easy to compute with the lattice code used to generate $G(t)$: simply recompute the correlator with the same code and lattice parameters, but replacing the gluon link matrices by the unit matrix everywhere. Moments of this gluon-free propagator are the $G_n^{(0)}$.

[22] We use the η_c mass because it is the easiest charmonium mass to measure accurately in a simulation, and because the experimental value is known to better than 0.1%.

[23] Using $m_{\eta_c}^{\rm exp}(am_c/am_{\eta_c})^{\rm LQCD}$ to determine m_c with reduced tuning errors is an old idea: see, for example, C. T. H. Davies *et al.*, Phys. Rev. Lett. **73**, 2654 (1994); A. Gray, I. Allison, C. T. H. Davies, E. Dalgic, G. P. Lepage, J. Shigemitsu, and M. Wingate, Phys. Rev. D **72**, 094507 (2005).

[24] We computed the contribution from c-quark loops by comparing results from [7] for $n_h = 1$ (with c quarks) with those for $n_h = 0$ (without c quarks). The reduced moments R_n are corrected, to include c quarks, by multiplying them by $r_n(n_h = 1)/r_n(n_h = 0)$.

[25] Note that configuration sets 3, 4, and 5 all have roughly the same lattice spacing, but the lattice for set 3 is 20% longer in each spatial direction than the others. Results from set 3 show no significant differences from those coming from the other two sets.

[26] One might worry about simulation errors in the calculation of m_{η_c} itself and their effect on m_{0c}. While statistical errors in m_{η_c} are negligible, there are certainly finite-a errors and some (weak) dependence on the sea-quark masses. These will induce additional finite-a and sea-quark mass dependence in other quantities, like our reduced moments, that depend upon m_{0c}. These additional terms are small, because our HISQ c-quark action is highly improved, and they are handled properly by the a^2 and chiral analysis of the reduced moments and other quantities of interest.

[27] In most lattice simulations one wants to tune the sea-quark masses to their physical values. Here, however, we extrapolate to zero mass in order to remove nonperturbative contributions proportional to the sea-quark masses. This extrapolation turns out to be almost negligible.

[28] G. P. Lepage, B. Clark, C. T. H. Davies, K. Hornbostel, P. B. Mackenzie, C. Morningstar, and H. Trottier, Nucl. Phys. B, Proc. Suppl. **106**, 12 (2002).

[29] For a detailed example of how to use constrained fitting, including how to construct an error budget for the results, and also for new results from lattice QCD for the QCD coupling see: C. T. H. Davies, I. D. Kendall, G. P. Lepage, C. McNeile, J. Shigemitsu, and H. Trottier (HPQCD Collaboration), arXiv:0807.1687.

[30] An alternative choice, $\mu = m_c(m_c)$, gives smaller perturbative coefficients for the moments of interest, but $\alpha_{\overline{\rm MS}}(\mu)$ is substantially larger. Consequently $\mu = 3$ GeV gives smaller errors than $\mu = m_c(m_c)$ despite having somewhat

larger expansion coefficients. Differences in the final results are small, however.

[31] This gives a perturbative error that is approximately the same size as the error estimates obtained in [2] by varying the renormalization scale between $\mu = 2$ and 4 GeV. The value for R_6, for example, varies from $+0.5\%$ to -0.4% of the central value as μ is varied over this range; the error estimate from Eq. (16) is $\pm 0.4\%$.

[32] V. A. Novikov, L. B. Okun, M. A. Shifman, A. I. Vainshtein, M. B. Voloshin, and V. I. Zakharov, Phys. Rep. **41**, 1 (1978).

[33] D. J. Broadhurst, P. A. Baikov, V. A. Ilyin, J. Fleischer, O. V. Tarasov, and V. A. Smirnov, Phys. Lett. B **329**, 103 (1994).

[34] For a recent analysis of condensate values see B. L. Ioffe, Prog. Part. Nucl. Phys. **56**, 232 (2006).

[35] T. van Ritbergen, J. A. M. Vermaseren, and S. A. Larin, Phys. Lett. B **400**, 379 (1997).

[36] M. Czakon, Nucl. Phys. **B710**, 485 (2005).

[37] K. G. Chetyrkin, Phys. Lett. B **404**, 161 (1997).

[38] J. A. M. Vermaseren, S. A. Larin, and T. van Ritbergen, Phys. Lett. B **405**, 327 (1997).

[39] Note that the error in $m_c(m_c) = 1.268(9)$ GeV is smaller than that in $m_c(\mu) = 0.986(10)$ GeV. This is because the scale in $m_c(m_c)$ is not fixed but rather varies as $m_c(m_c)$ itself is varied across the interval 1.268 ± 0.009 GeV.

[40] W.-M. Yao *et al.* (Particle Data Group), J. Phys. G **33**, 1 (2006); We use the Particle Data Group's value of $m_b(m_b) = 4.20(7)$ GeV for the b-quark mass when reducing from $n_f = 5$ to $n_f = 4$.

[41] A related problem is that correlators built from these currents are contaminated by contributions from correlators built from opposite-parity operators (see Appendix G of [14]). These lattice artifacts oscillate in sign, as $(-1)^{t/a}$, and so are suppressed by $(am_c/\pi)^{n-2}$ in the nth moment since the sum over t is dominated by $E \approx 0$. Such contamination is absent in the case of the pseudoscalar correlators.

[42] We fit these reduced moments the same way we fit the pseudoscalar moments except that we need a prior $\sigma_c = 2$ for the $c_{n,i}$ that is twice as wide.

[43] The continuum Ward identity relates the axial vector current to the pseudoscalar density [52], implying that $g_n^{(j_{5\mu})} \propto g_{n+2}$ where the g_n's are defined in Eqs. (4) and (26).

[44] For older analyses that include sea quarks, see: A. Dougall, C. M. Maynard, and C. McNeile, J. High Energy Phys. 01 (2006) 171; M. Nobes and H. Trottier, Proc. Sci., LAT2005 (2006) 209.The precision of analyses that do not include sea quarks is hard to quantify because the value of the c mass depends upon how the lattice spacing and the bare c mass are tuned, and it is not possible to obtain consistency from different choices. For example, tuning the bare mass to give the correct D_s mass gives very different results from tuning to get the correct $D_s^* - D_s$ mass difference, or the correct η_c or ψ mass. We avoid these problems here by including the full effect of sea quarks. For determinations of the c mass without sea quarks with further discussion of these issues see: J. Rolf and S. Sint (ALPHA Collaboration), J. High Energy Phys. 12 (2002) 007; G. M. de Divitiis, M. Guagnelli, R. Petronzio, N. Tantalo, and F. Palombi, Nucl. Phys. **B675**, 309 (2003).

[45] A world average of 0.1189(10) is given in S. Bethke, Prog. Part. Nucl. Phys. **58**, 351 (2007).

[46] S. R. Sharpe, Proc. Sci., LAT2006 (2006) 022.

[47] C. Bernard, M. Golterman, Y. Shamir, and S. R. Sharpe, Phys. Rev. D **77**, 114504 (2008).

[48] K. M. Ecklund *et al.* (CLEO Collaboration), Phys. Rev. Lett. **100**, 161801 (2008).

[49] M. Artuso *et al.* (CLEO Collaboration), Phys. Rev. Lett. **99**, 071802 (2007).

[50] B. Aubert *et al.* (*BABAR* Collaboration), Phys. Rev. Lett. **98**, 141801 (2007).

[51] HPQCD Collaboration (unpublished).

[52] D. J. Broadhurst, Phys. Lett. **101B**, 423 (1981).

[53] Details of the calculation, as well as analytical results, will be presented in C. Sturm (unpublished).

[54] A. Maier, P. Maierhofer, and P. Marqaurd, arXiv:0806.3405.

[55] M. Czakon and T. Schutzmeier, J. High Energy Phys. 07 (2008) 001.